Geochemistry Geophysics Geosystems G3
AN ELECTRONIC JOURNAL OF THE EARTH SCIENCES
Published by AGU and the Geochemical Society

Article
Volume 9, Number 10
21 October 2008
Q10Z01, doi:10.1029/2008GC002110
ISSN: 1525-2027

Morin transition in hematite: Size dependence and thermal hysteresis

Özden Özdemir and David J. Dunlop
Chemical and Physical Sciences, University of Toronto, Mississauga, Ontario L5L 1C6, Canada (ozdemir@physics.utoronto.ca)

Thelma S. Berquó
Institute for Rock Magnetism, University of Minnesota, Minneapolis, Minnesota 55455, USA

[1] Hematite is a frequently used mineral in paleomagnetic and environmental magnetic studies. Just below room temperature, it undergoes a magnetic phase transition, the Morin transition, whose nature is an important part of our basic understanding of hematite's magnetism and magnetic memory. We have determined the temperature T_M of the Morin transition from saturation remanence warming curves to be 250–261 K for 0.5–6 mm hematite natural single crystals, 257–260 K for 45–600 μm sieved crystal fractions, and 241–256 K for submicron synthetic hematites with grain sizes between 120 and 520 nm. The variation must be due to differences in crystal morphology, lattice strain, and crystal defects common in both synthetic and natural crystals. Our results are compatible with published data for 100 nm to 10 mm hematites and show that T_M is nearly size independent, decreasing very gradually as particle size decreases over this broad range, which includes both multidomain (MD) and single-domain (SD) structures. However, T_M decreases sharply between 90 and 30 nm. Below 20 nm, the transition disappears entirely as near-surface spins deviate strongly from the antiferromagnetic easy axis. Our SD and MD hematites exhibit a thermal hysteresis in the Morin transition: the values of T_M in cooling and in heating are different. For the same cooling/warming rate, ΔT_M is much greater for submicron hematites than for larger crystals. We attribute the lag in the transition in both cooling and heating to crystal imperfections and resulting internal stresses, and speculate that defects may serve to pin and stabilize surface spins. Preventing spin rotation in a region large enough to trigger the phase transition would inhibit destabilization of the weakly ferromagnetic phase in cooling and the antiferromagnetic phase in heating. The wide distribution of particle sizes in our submicron samples may also play a role.

Components: 6959 words, 8 figures.

Keywords: hematite; Morin transition; thermal hysteresis; low-temperature properties.

Index Terms: 1540 Geomagnetism and Paleomagnetism: Rock and mineral magnetism; 1519 Geomagnetism and Paleomagnetism: Magnetic mineralogy and petrology; 1512 Geomagnetism and Paleomagnetism: Environmental magnetism.

Received 28 May 2008; **Revised** 15 August 2008; **Accepted** 28 August 2008; **Published** 21 October 2008.

Copyright 2008 by the American Geophysical Union

Özdemir, Ö., D. J. Dunlop, and T. S. Berquó (2008), Morin transition in hematite: Size dependence and thermal hysteresis, *Geochem. Geophys. Geosyst.*, *9*, Q10Z01, doi:10.1029/2008GC002110.

Theme: Magnetism From Atomic to Planetary Scales: Physical Principles and Interdisciplinary Applications in Geoscience
Guest Editors: J. Feinberg, F. Florindo, B. Moskowitz, and A. Roberts

1. Introduction

[2] Hematite has a magnetic phase transition, the *Morin* [1950] transition, at $T_M \approx 250$ K. Below T_M, spins lie along the trigonal or c axis of the rhombohedral lattice, equal numbers in either orientation. This antiferromagnetic (AF) structure changes to weakly ferromagnetic (WF) on heating through T_M, as spins flop 90° to the basal c plane, within which they are canted out of exact antiparallelism by a fraction of a degree. The c axis and basal plane spin orientations were first demonstrated by *Shull et al.* [1951] in an early neutron diffraction study. Spin flopping arises from the competition between dipolar ($K_{MD} < 0$) and single-ion ($K_{SI} > 0$) anisotropies. K_{SI} dominates at low temperature and the spins lie along the trigonal axis. As temperature T rises, K_{SI} falls more rapidly than K_{MD}, which favors basal plane spin alignment, and a spin flop transition occurs at T_M. Magnetic field, pressure, particle size, and lattice strain originating in crystal defects all affect the balance between K_{MD} and K_{SI} and shift T_M.

[3] The earliest [*Morin*, 1950] and still the commonest way of studying the Morin transition is using susceptibility and remanence measurements. Morin reported that the transition was suppressed by the addition of 1% Ti to the lattice. *Haigh* [1957a, 1957b] studied pure and Ti- and Al-substituted hematites using an astatic magnetometer and discovered the memory effect, a partial recovery of remanence in thermal cycles across T_M. *Muench et al.* [1985] used a vibrating-sample magnetometer to study the transition as a function of grain size and applied magnetic field in synthetic submicron hematites. *Zysler et al.* [2003], using a SQUID magnetometer, found that both T_M and the spin flop transition field increase with increasing crystallite size in acicular hematite nanoparticles. SQUIDs permit higher resolution measurements of hematite's weak canted ferromagnetism and are now in general use in the rock magnetic community [*de Boer et al.*, 2001].

[4] Torque magnetometer data determine hematite's anisotropy constants. *Flanders and Schuele* [1964] reported a weak triaxial anisotropy in the basal plane of natural hematite crystals with anisotropy constants of 7–188 ergs/cm^3. Using a similar magnetometer, *Flanders* [1969] deduced a three-step process for rotation of spins from [111], the AF c axis, into (111), the WF plane, as $H_\perp$ and/or T increase. The rotation starts with a smooth change in θ, increasing in rate for higher T; this is followed by an abrupt jump; finally as θ approaches 90°, there is a smaller, more gradual jump.

[5] Mössbauer spectroscopy (MS) has frequently been used to study the Morin transition, magnetic structure, and superparamagnetism (SP) in hematite [*Kündig et al.*, 1966; *Schroeer and Nininger*, 1967; *Donbaev et al.*, 1993; *Dang et al.*, 1998; *Vandenberghe et al.*, 2001]. *Ruskov et al.* [1976] examined single crystals and polycrystalline samples, with and without an external magnetic field in the basal plane, and concluded that spin rotation at the Morin transition takes place with a jump. *Nininger and Schroeer* [1978], measuring MS of microcrystalline (5–75 nm) and reference bulk hematites at the Morin transition, were able to resolve the spectra of coexisting WF and AF phases. The transition in bulk hematite occurred over <0.4 K. In microcrystals, T_M decreased linearly with expanding lattice, in agreement with the increase of T_M under external pressure.

[6] After shock loading at pressures from 8 to 27 Gpa, MS revealed drastically altered behavior [*Williamson et al.*, 1986]. Many Fe sites no longer exhibited a transition and those that did had reduced T_M and increased thermal hysteresis. The Mössbauer quadrupole splitting indicated <90° spin rotation at T_M for the higher pressures. The observed effects are due to reduced crystallite size and/or residual strain associated with high defect densities.

[7] Using MS, *Sorescu et al.* [1999] detected variable amounts, depending on particle morphol-

ogy, of WF hematite coexisting with the AF phase below T_M = 230 K. *Bødker et al.* [2000] found that 16 nm nanoparticles are WF at least down to 5 K, with spontaneous magnetization slightly higher than that of bulk polycrystalline (>3 μm crystals) hematite. They distinguished two different modes of SP relaxation of the WF phase. The first, rotation of sublattice magnetization directions in the basal plane, gives rise to SP behavior in MS. The other, involving fluctuations of the net magnetization vector out of the basal plane, mainly affects magnetization measurements. Finally, *Frandsen and Mørup* [2005] found that for agglomerated particles, interparticle interactions can rotate the sublattice magnetizations up to 15° out of plane, depending on particle size.

[8] Spin arrangements near T_M can be obtained using neutron diffraction. *Shull et al.* [1951] established that the magnetic moments lie in (111) above T_M and along [111] below T_M. *Morrish et al.* [1963] measured a residual (111) intensity below T_M, which they attributed to a 10° tilt of the spins away from the c axis. *Nathans et al.* [1964] and *Hönigschmid and Will* [1979] also detected a small basal plane or WF component below T_M.

[9] Neutron scattering is sensitive to magnetic relaxation processes with characteristic times of 10^{-13}–10^{-10} s and is therefore very useful in studying relaxation in nanoparticles [*Hansen et al.*, 1997; *Klausen et al.*, 2003; *Kuhn et al.*, 2006]. *Frandsen et al.*, [2005] studied chains of 5–10 nm hematite nanoparticles attached along a common [001] axis. Neutron diffraction studies on two- to five-particle chains show both structural and magnetic correlations across interfaces along the [001] direction, evidence of exchange coupling between particles. An exchange-coupled chain behaves as a single particle; in particular, SP relaxation is suppressed.

[10] Neutron diffraction topography [*Baruchel et al.*, 1987] indicates that the Morin transition takes place through a succession of abrupt transitions of regions of the sample and gives images of these regions, which may be related to crystal imperfections.

[11] *Parpia et al.* [1987] used synchrotron radiation topography to investigate the Morin transition in flux-grown crystals. Domain boundaries were revealed in the topographs of some crystals at temperatures as low as 77 K, much below T_M. WF and AF phases coexisted over a wide temperature range and T_M itself varied greatly with specimen perfection. *Schetinkin et al.* [2003] also observed WF and AF phase coexistence in single-crystal hematite during spin reorientation at the Morin transition. The WF-AF phase boundaries moved while remaining nearly parallel to (111). Nucleation of the WF phase and pinning of interphase boundaries on defects in the crystal were also observed, confirming observations made by *Gallon* [1968] in the region of the Morin transition using Bitter colloid patterns.

[12] Acoustic methods involving compressional and shear waves are another way to study the Morin transition. When an elastic wave propagates through a magnetic material, the alternating elastic deformations drive magnetostrictive oscillations of the domain walls. Frictional forces damp the domain wall motion, causing the sound wave to lose energy. *Shapira* [1969] observed a sharp peak in attenuation at T_M = 260.6 K for a pure natural single crystal of Brazilian hematite. He also observed anomalies in attenuation near the transition in fields parallel and perpendicular to the trigonal axis and used these to determine the critical fields $H_{C\perp}$ = 160.8 ± 2 kG and $H_{C\parallel}$ = 68.2 ± 0.7 kG required for spin flopping. *Liebermann and Banerjee* [1971] likewise reported large increases in attenuation and decreases in velocities of ultrasonic waves in hematite caused by magnetoelastic domain wall-stress interaction.

[13] Magnetooptical effect [*Le Gall et al.*, 1977], differential thermal analysis [*Gallagher and Gyorgy*, 1969], and magnetic resonance [*Anderson et al.*, 1954] are other techniques used to study the Morin transition.

[14] In the present paper, we use magnetization measured by a SQUID magnetometer in the course of zero-field thermal cycling of saturation isothermal remanent magnetization (SIRM) to determine the Morin transition temperature T_M. We report T_M in both warming and cooling as a function of grain size and applied magnetic field.

2. Sample Characterization

[15] We used three sets of synthetic submicron hematites with sizes in the single-domain (SD) range [*Özdemir and Dunlop*, 2002]. The first set was prepared by heating cube-shaped magnetite crystals at 700°C in air for 18 h. Their average grain sizes range between 0.12 and 0.23 μm. The second set consists of Pfizer™ hematite powders heated in air for 5 h at 500°C to oxidize any magnetic impurities. Median particle sizes after

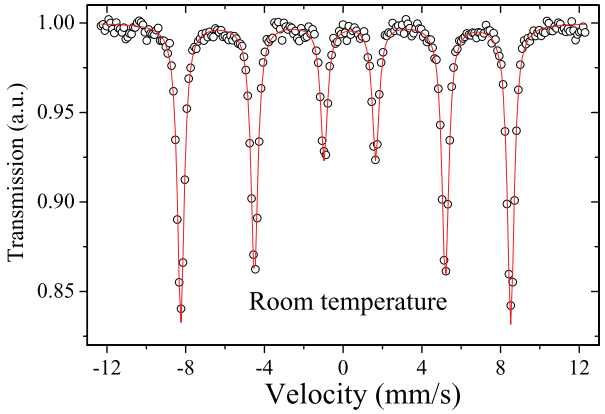

Figure 1. Room temperature ^{57}Fe Mössbauer spectrum (transmission expressed in linear-scale γ ray counts versus Doppler velocity) of one of the Brazilian hematite samples. Fitting of the spectrum was carried out using a single standard hematite component [*Murad and Cashion*, 2004]. There is no other Fe phase present. The hyperfine parameters also match those of stoichiometric hematite (see text).

heat treatment were 0.14–0.42 μm. The third set was obtained by heating Pfizer™ magnetite, maghemite, and lepidocrocite at 700°C for 19 h. The heated magnetites and maghemites have rounded forms with average sizes from 0.35 to 0.45 μm. The heated lepidocrocite produced acicular particles of average diameter 0.06 μm and length 0.52 μm. X-ray analysis using a Siemens D5000 diffractometer with Co Kα radiation gave well-defined hematite diffraction patterns free of iron impurities.

[16] We also studied fourteen crystals, basal plane platelets with (111) faces between 1 mm × 2 mm and 3.7 mm × 5.5 mm in size and thicknesses of 0.14–1.0 mm, cleaved from natural single crystals of hematite from Mount Wright, Québec, Canada; Rio Marina, Elba, Italy; and Bahia, Brazil [*Özdemir and Dunlop*, 2005]. A powder of smaller crystals from Minas Gerais, Brazil was sieved into seven fractions: <45 μm, 45–63 μm, 63–90 μm, 90–125 μm, 250–355 μm, 355–500 μm, and 500–710 μm. All crystals are of multidomain (MD) size.

[17] Scanning electron microscopy (Hitachi S570) with energy dispersive X-ray microanalysis (EDAX LZ-5) on representative single crystals from each location indicated stoichiometric hematite with no major impurities. High-field thermomagnetic curves measured with a Princeton Measurements vibrating-sample magnetometer gave hematite Néel temperatures of 680–690°C for SD and 679–696°C for natural MD hematite crystals.

[18] Mössbauer spectroscopy was carried out at room temperature using a constant-acceleration spectrometer in transmission geometry with a ^{57}Co/Rh source. Isomer shifts and velocity scale were calibrated using αFe. The Mössbauer spectrum of one of the Brazilian samples (Figure 1) was fitted with only one component. The fitted lines agree with those of standard hematite [*Murad and Cashion*, 2004]; no other iron phase is present and no relaxation indicating fine particle size was seen. The hyperfine parameters match those of stoichiometric hematite: magnetic hyperfine field B_{HF} = 51.8(1) T; quadrupole splitting QS = – 0.21(1) mm/s; and isomer shift IS = 0.37(1) mm/s. The value of B_{HF} indicates that the hematite is very well crystallized, without isomorphic substitution or structural defects. Negative QS values for spectra taken above the Morin transition are typical of canted antiferromagnetism in hematite.

3. Experimental Results

3.1. SIRM Cooling-Warming Cycles

[19] Hematites were given a 2.5-T SIRM at 300 K, then cooled to 20 K and warmed back to 300 K in zero field. Magnetization was measured at 5 K (≈1 min) intervals with a Quantum Design MPMS-2 SQUID magnetometer (residual field ≈10 μT). In single crystals, SIRM was produced in the (111) plane. SIRM cooling/warming cycles are useful in determining the Morin transition temperature T_M and its thermal hysteresis and also provide information about magnetic memory and the "defect moment" (the WF moment below T_M).

[20] Typical cooling and warming curves of 300-K SIRM for submicron SD and natural MD single crystal samples appear in Figures 2 and 3. SIRM of an acicular SD hematite decreases continuously between 300 and 250 K and then largely vanishes between 250 and 235 K with the disappearance of spin-canting. We obtain a value T_M = 239 K by projecting the steepest part of the remanence decrease, in this case between the 245 and 240 K data points, to intersect the projection of the line defined by the 230–20 K data. This data plateau, the low-temperature remanence or defect moment surviving below T_M, is only 2% of the 300-K SIRM. As the crystal warms from 20 K, the remanence retraces the cooling curve but the onset of the Morin transition to the WF state is delayed by about 10 K: T_M = 249 K in warming.

[21] This thermal hysteresis is not due to temperature lag. The heating rate of ≈5 K/min is slow

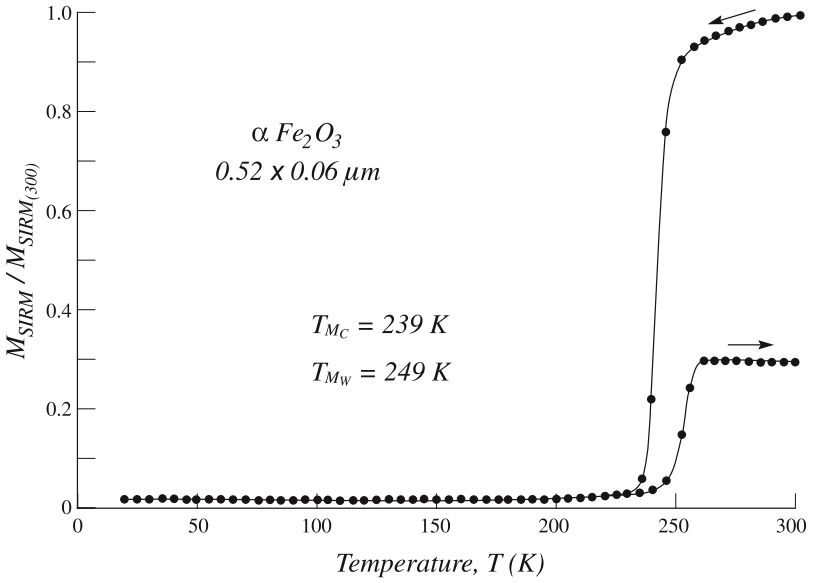

Figure 2. Zero-field thermal cycling of room temperature SIRM for a sample containing acicular SD hematite particles. The Morin transition is quite broad, covering a range of >10 K and occurs at lower temperatures in cooling than in heating (thermal hysteresis). Extrapolating the tangent of steepest descent/ascent to intersect the projected remanence below T_M gives estimates of 239 K in cooling and 249 K in warming. Although the remanence of the AF phase below T_M is very small, about one-third of the initial SIRM is regenerated as memory on warming through the transition.

enough to allow effective thermal equilibration. Moreover the larger single-crystal sample of Figure 3 has almost no thermal hysteresis: T_M = 254 K in cooling and 256 K in warming.

[22] The cooling and warming curves of the SD and MD samples are remarkably similar, implying that domain structure has little to do with the remanence loss and recovery (memory) phenomena in hematite. The main differences visible in Figure 3 are that the WF moment scarcely decreases in cooling from 300 to 270 K and the WF → AF transformation between 265 and 255 K

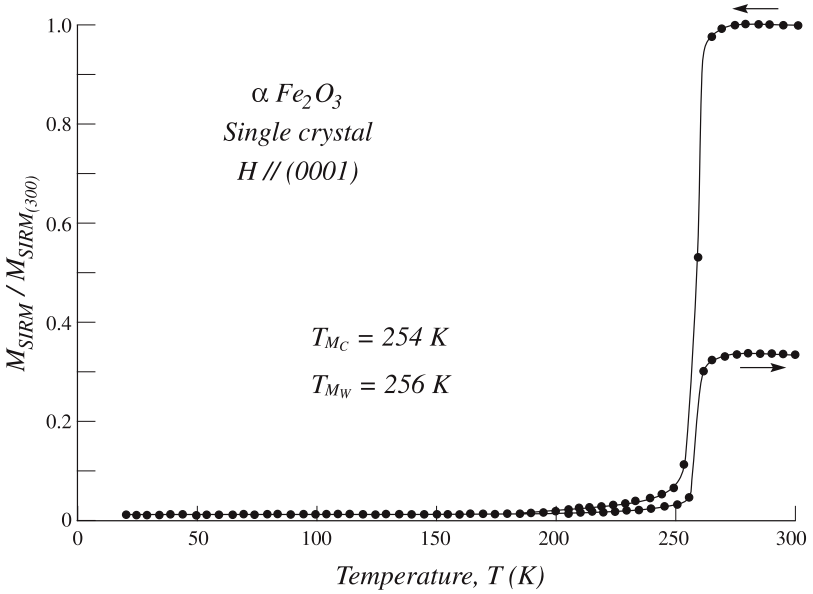

Figure 3. Zero-field thermal cycling of room temperature SIRM produced in the basal plane of a millimeter-size single crystal of hematite. The Morin transition is much sharper than in Figure 2, covering a range of 5–7 K in both cooling and heating. Thermal hysteresis ΔT_M is only 2 K, much less than for most SD samples. Despite the differences in domain structure and other magnetic properties, the low-temperature AF moment and room temperature memory of initial SIRM are similar to those of the SD sample of Figure 2.

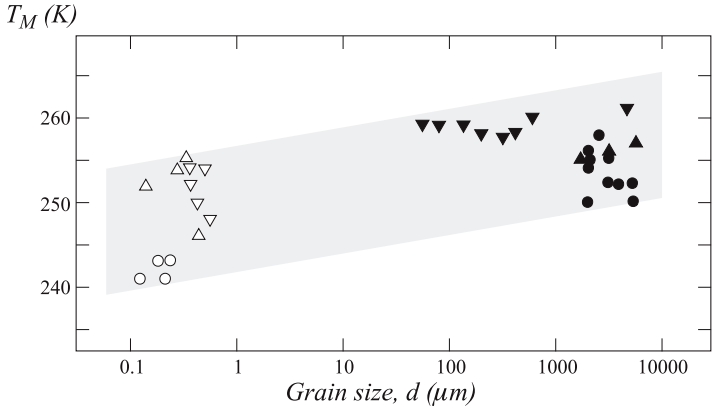

Figure 4. A compilation of T_M values (from warming curves) for submicron synthetic hematites (open symbols: circles, set 1; upright triangles, set 2; inverted triangles, set 3) and natural hematite crystals (solid symbols: circles, Québec; upright triangles, Rio Marina, Elba; inverted triangles, Bahia and Minas Gerais, Brazil). MD single crystals, particularly those of common provenance, have narrower ranges of T_M values which are higher on average than those of SD synthetic hematites. The four SD hematites of set 1 may owe their low T_M values in part to size distributions extending below 90 nm, a range in which T_M falls rapidly because of surface effects (cf. Figure 8).

is somewhat sharper than in the SD case. The reverse transformation on heating is also more abrupt than in the SD case. Otherwise the SD and MD results are very comparable. The low-temperature moment, nominally zero in the AF phase, is again about 2% of 300-K SIRM. The remanence recovered at room temperature is 30% of the original SIRM in Figure 2 and 33% in Figure 3. This memory phenomenon presumably originates in coupling between WF nuclei below T_M and the full spin-canted phase above T_M [*Özdemir and Dunlop*, 2005, 2006].

3.2. Morin Transition Temperature T_M

[23] Our Morin transition temperature data are summarized in Figure 4. T_M is quite variable in both SD and MD hematites. Submicron hematites have lower T_M values on average, ranging from 241 to 256 K (values from heating curves). Fine particle size and associated internal strains lower the transition temperature [*Muench et al.*, 1985]. The broad range of T_M in synthetic hematites may also be due to different methods of preparation, crystal morphology, degree of crystallinity, and nonmagnetic impurities. Closely related samples prepared by heating cube-shaped magnetite crystals grown from aqueous solution (open circles in Figure 4) have T_M values tightly grouped between 241 and 243 K, reflecting their similar defect densities and purities.

[24] Natural single crystals have higher T_M on average; individual values range from 250 to 261 K. T_M values for Brazilian hematite sieve fractions are narrowly distributed between 257 and 260 K, reflecting the common origin and presumably similar defect densities of these platelets. The broader range (10 K) of T_M for the Québec and Rio Marina hematites must be due to greater variation in types and populations of crystal defects. The commonest crystal imperfections in hematites are growth and deformational twins, twin boundaries, line and planar defects, e.g., screw dislocations, and irregularities such as misoriented crystals. These defects produce a stress-strain distribution in the crystal and affect the balance between the competing dipolar and single-ion anisotropies that control the Morin transition temperature.

3.3. Thermal Hysteresis and ΔT_M

[25] Our SD and MD hematites have variable amounts of thermal hysteresis, i.e., temperature lag in the reorientation of spins parallel or perpendicular to the c axis at the Morin transition. SD samples had particularly sluggish phase transitions (Figure 5). The WF → AF transformation in cooling occurred 6–18 K below the AF → WF transformation temperature on warming. For MD samples, the differences between T_M in cooling and warming were 1–9 K (Figure 5), most Québec and Brazilian crystals having $\Delta T_M < 5$ K.

[26] The hysteresis width ΔT_M is clearly much larger in most submicron hematites than in MD-size natural crystals. This variation in ΔT_M may be related to the wide distribution of particle sizes. The sieved Brazilian hematites are narrowly sized and have very small ΔT_M values of 1–3 K. Most

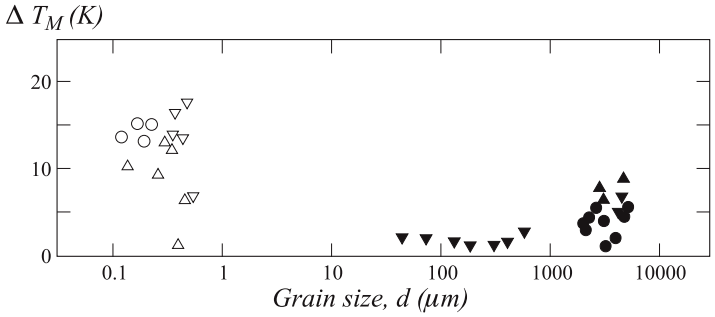

Figure 5. A compilation of thermal hysteresis widths ΔT_M determined as the difference between T_M values in heating and cooling. Sample symbols as in Figure 4. ΔT_M values are much larger for most SD samples than for the Brazilian and Québec single crystals.

submicron samples, on the other hand, have broader size distributions after heat treatment. As well as size distribution, another possible factor could be defect density. Heat treatment during sample preparation degrades the crystallinity of the synthetic hematites, most of which have large ΔT_M values. However, the samples of set 1, which originated as hydrothermal (low-stress) magnetites, have ΔT_M values around 15 K, while about half the samples from the other two sets have ΔT_M values of 10 K or less.

[27] Thermal hysteresis loops were measured in the (111) plane of a 0.12 × 1.4 × 2 mm Québec single crystal using a low-temperature microVSM (Figure 6). Fields ranging from 0.1 T to 1.5 T were applied during thermal cycling similar to that illustrated in Figures 2 and 3, except that there was no initial SIRM. The lowest loop, for $H = 0$, is different in that an initial SIRM was produced before cooling began. Shading is used in the figure to emphasize the offset between cooling and warming curves. In Figure 7, the Morin transition temperatures determined from the cooling and warming curves, as described in section 3.1, are plotted as a function of field H. The Morin transition temperature is field dependent and decreases with increasing field intensity. However, the thermal hysteresis offset ΔT_M of the transition, 4 K for this sample, is independent of the field applied.

4. Discussion

4.1. Size Dependence of T_M

[28] Literature values for the Morin transition temperatures of a wide variety of synthetic and natural hematites are compared in Figure 8 with our (warming) T_M values. T_M values were obtained from remanent magnetization, magnetic susceptibility, torque measurements, Mössbauer spectroscopy, neutron diffraction, synchrotron radiation, and ultrasonic absorption data. Our T_M data for submicron SD grains and MD single crystals are generally consistent with values for other synthetic and natural hematites, despite the heterogeneity of origins and sample treatments.

[29] The data in Figure 8 follow two trends. In nanoparticles with sizes from 30 to 100 nm, T_M is strongly dependent on particle size. In the broad range from 100 nm to 10 mm, which includes both SD and MD structures, T_M is weakly size dependent, on average increasing slightly with increasing grain size. This size trend is most convincingly seen in the three data points of *Kletetschka and Wasilewski* [2002] in the intermediate size range close to and above the SD-MD threshold. There are numerous examples, however, of smaller T_M values for large MD grains and larger T_M values for submicron SD grains which run counter to the general trend.

4.1.1. The 30–100 nm Range

[30] T_M decreases very sharply in nanoparticles with sizes below 100 nm, dropping to ≈190 K by 30 nm (Figure 8), below which size the Morin transition disappears [*Bando et al.*, 1965; *Klausen et al.*, 2003]. Note that 30 nm is close to the room temperature SP threshold of 27.5 nm for the WF phase [*Banerjee*, 1971] at which SD moments become excited thermally on a timescale of seconds. *Bødker et al.*'s [2000] observation that 16 nm nanoparticles are WF at least down to 5 K confirms that no Morin transition is present in these ultrafine hematites. Presumably, it is the much smaller SP threshold size on Mössbauer timescales that makes this observation possible.

[31] Why does T_M decrease in nanoparticles? As particle size decreases, surface-to-volume ratio

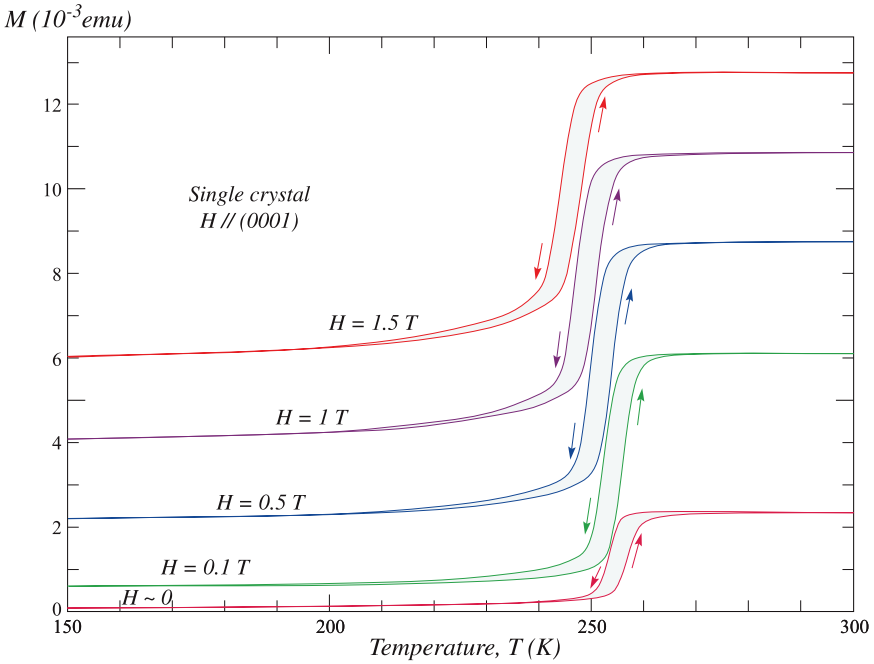

Figure 6. Thermal hysteresis exhibited by cycling a Québec single crystal in the presence of fields ***H*** of different strengths applied in the basal plane (no initial SIRM), compared to the hysteresis of the cooling and warming curves of initial SIRM in zero applied field. Shading has been applied to emphasize the hysteresis but has no physical significance. The Morin transition is displaced to lower T as H increases but the hysteresis width ΔT_M remains a constant 4 K.

increases and surface effects come to dominate the magnetic properties. Lower lattice symmetry and broken bonds at the crystal surface give rise to spin disordering or deviation from antiferromagnetic alignment. Rotation of sublattice magnetizations by ≈15° has been detected by Mössbauer measurements on 8–9 nm agglomerated particles [*Frandsen and Mørup*, 2005]. These particles have no Morin transition and are in the WF state at all temperatures. In 40 nm spherical hematites with T_M = 220 K, *Gee et al.* [2004] observed that the spins flop from 90° to 28° (the [110] axis), not 0° (the [111] axis), in cooling through the Morin transition. The usual 90° spin flopping is compro-

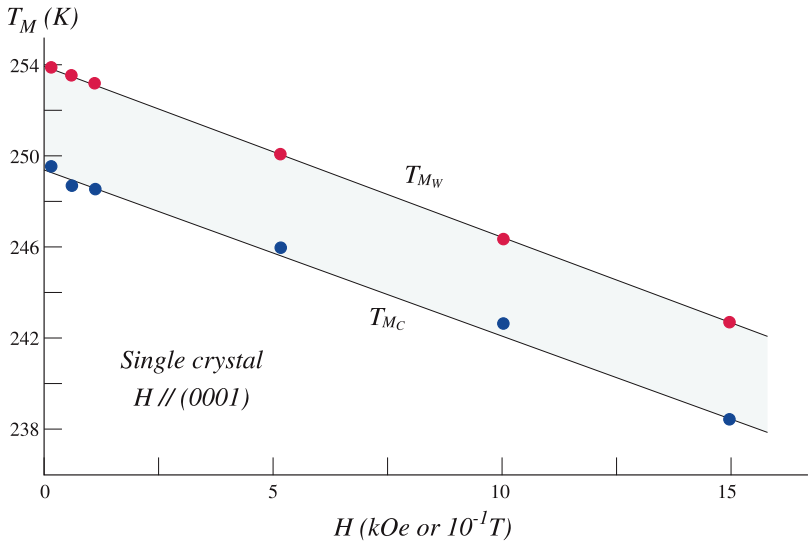

Figure 7. Linear decrease of the Morin transition temperatures in warming and cooling with increasing applied field H. Shading has been applied to emphasize the constant hysteresis width ΔT_M.

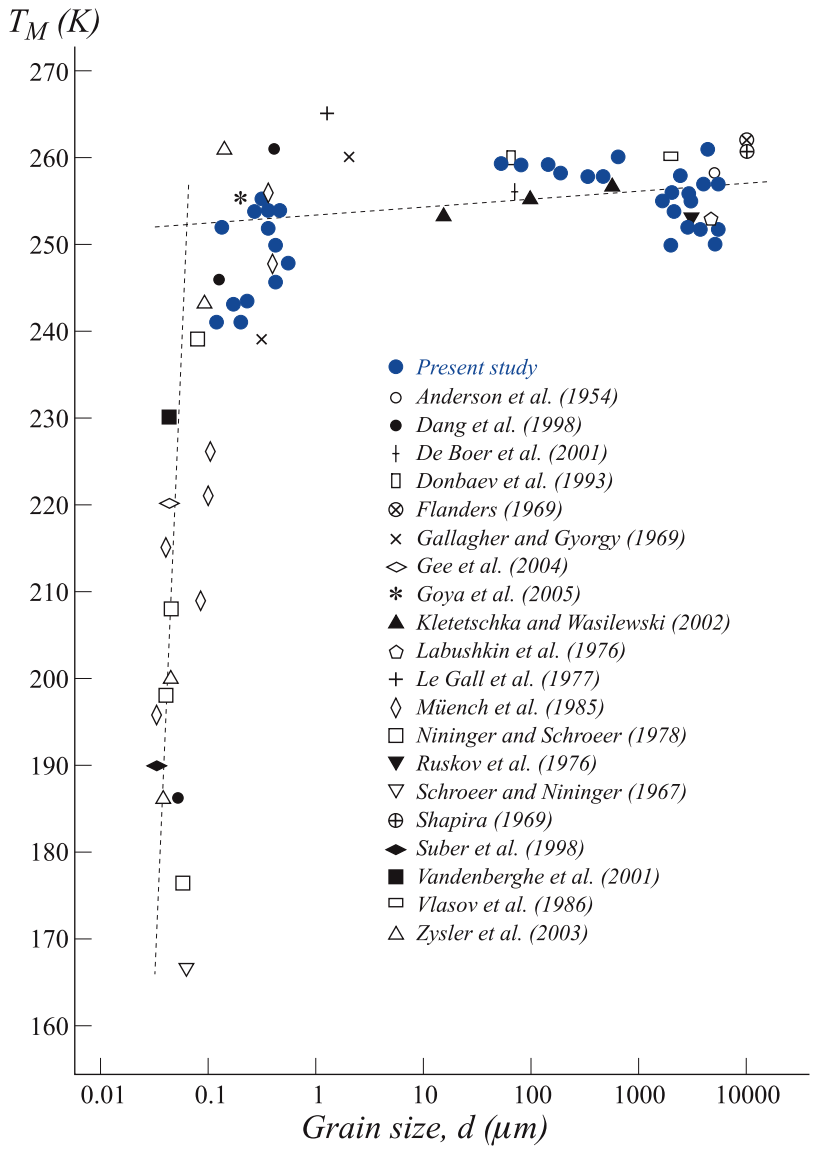

Figure 8. Values of T_M reported in the literature compared with our data set. The scatter is largely due to the variety of techniques used, lack of standardization in determining reported values of T_M, e.g., warming versus cooling values, and the heterogeneous nature of the samples examined. Two trends are clear, however. Samples with mean particle sizes between about 90 and 30 nm have depressed (in some cases greatly depressed) Morin transitions, with T_M values from 230 K to as low as 165 K. Samples with mean sizes from 100 nm to 5 mm have hardly any variation in the Morin transition temperature. Except for some of the finest SD samples which probably include a <100 nm fraction, T_M in this broad size range is typically between 250 and 260 K and seems to be an intrinsic material property, dependent only on the spin sublattices and independent of domain structure.

mised in these much larger particles, suggesting that surface anisotropy is already seriously upsetting the balance between dipolar and single-ion anisotropies.

4.1.2. The 100 nm to 10 mm Range

[32] The Morin transition temperature is generally stated to be ≈260 K in bulk hematite and to decrease as particle size is reduced [*Flanders*, 1969; *Shapira*, 1969]. Examining the large data set of Figure 8 makes it clear that values of T_M are in fact widely dispersed throughout the 100 nm to 10 mm range. MD hematites of mm size have T_M values ranging from 250 to 260 K, which is greater than (about double) the decrease in average T_M between 10 mm and 100 nm. T_M ranges even more widely in submicron SD hematites, from 238 K to 260 K. The lowest values, from 238 to 245 K, are for the finest sizes and may reflect <100 nm fractions in sample size distributions.

[33] At least some of the scatter in the data is the result of factors other than grain size. The first is thermal hysteresis. T_M is different when the Morin transition is approached from below (AF state) rather than above (WF state). The direction of approach is not always clear in published studies, nor is the field applied, which also affects the Morin transition. Our results show that T_M decreases substantially, by about 10 K, as the applied field increases from 0 to 1.5 T for both SD and MD hematites (Figures 6 and 7). For this reason, our T_M data (Figures 2, 3, 4, and 8) were determined in zero applied field. *Muench et al.* [1985], *Amin and Arajs* [1987], and *Suber et al.* [1998] also reported linear decreases of T_M with increasing applied field.

[34] Another factor affecting the Morin transition temperature is heat treatment [*Muench et al.*, 1985; *Amin and Arajs*, 1987; *Suber et al.*, 1998]. *Zysler et al.* [2003] show that T_M increases with increasing annealing temperature. Using TEM and X-ray diffraction they observed that thermal treatment resulted in grain growth which in turn increased T_M. Heat treatment also anneals out crystal defects and reduces internal strain, both of which affect the Morin transition temperature. Even small amounts of most impurity cations lower T_M [*Morin*, 1950; *Haigh*, 1957a] and the purity of experimental samples is often not specified in published studies. Finally, particle morphology and degree of crystallinity can alter both T_M and the sharpness or range of temperatures over which the transition occurs.

4.2. Thermal Hysteresis ΔT_M

[35] Different values of T_M in heating and cooling have been reported by *Flanders* [1969], *Labushkin et al.* [1976], *Nininger and Schroeer* [1978], *Muench et al.* [1985], *Vlasov et al.* [1986], *Williamson et al.* [1986], *Zysler et al.* [2003], *Goya et al.* [2005], and *Bercoff et al.* [2007]. *Williamson et al.*'s [1986] Mössbauer spectra of hematite powders shocked at pressures of 8 to 27 GPa showed an increase in thermal hysteresis from ΔT_M = 12 K for unshocked powder to ΔT_M = 45 K for the 17-Gpa sample. Increased thermal hysteresis was attributed to reduced crystallite size and the large defect density associated with residual strain following shock.

[36] *Vlasov et al.* [1986] proposed that crystal imperfections such as inclusions, dislocations, or nonstoichiometry can create nucleation centers for the magnetic phases. A metastable state of the AF (WF) phase beyond T_M on warming (cooling) would only be observed in nearly defect-free crystals where nucleation is difficult. Although this sounds reasonable, it runs counter to *Williamson et al.*'s [1986] observations of greatly increased ΔT_M values in shocked hematites. It also is not obviously borne out by our data. In Figure 5, synthetic hematites that have been heated merely to remove any unoxidized material have smaller ΔT_M values than hematites converted from magnetite, maghemite, or lepidocrocite. These latter hematites logically should contain more crystal imperfections but they in fact have larger ΔT_M values.

[37] *Goya et al.* [2005] observed thermal hysteresis in both structural and magnetic hyperfine parameters when 200 nm synthetic hematite crosses the Morin transition during heating or cooling. They appealed to magnon softening at the particle surface as the trigger for the phase transition. In the model proposed by *Chow and Keffer* [1974], surface magnons soften, depending on the local surface anisotropy, as the transition is approached from either below or above. The near-surface spins rotate and serve as nucleation centers that generate the transition throughout the entire crystal; the transition occurs when the free energies of the AF and WF states are equal.

[38] *Chow and Keffer*'s [1974] surface regions consist of 10^2 to 10^3 layers, a small fraction of a large MD crystal but a large fraction, if not the entire particle, in 30–90 nm particles. *Morrish* [1994] suggests that thermal hysteresis in the Morin transition is most often observed for small particles because all or most of the atoms are effectively "at the surface." If there are insufficient numbers of surface atoms to form a viable nucleating layer, the transition will be inhibited in both cooling and heating. Morrish speculates that thinner surface layers plus regions in the vicinity of imperfections or impurities may suffice to inhibit the transition. In this scenario, crystal defects would have a stabilizing rather than a triggering effect, which is more in line with the observations than *Vlasov et al.*'s [1986] model.

5. Conclusions

[39] Observed Morin transition temperatures are quite variable. Submicron SD hematites have lower T_M values, from 241 to 256 K. This broad range of T_M values is due in part to different methods of preparation, crystal morphology, crystallinity, and impurities. The finest samples, 100–200 nm in particle size, have the lowest T_M values: 241–

245 K. Their size distributions probably extend below 90 nm into a range where surface effects become important and T_M falls rapidly.

[40] Natural single crystals have higher T_M values and a narrower range of T_M values: 250–261 K. Natural hematites have a variety of crystal imperfections such as growth and deformational twins, twin boundaries, dislocations, and resulting internal stress which could alter T_M. The transition tends to be quite sharp in MD grains and broader in SD grains.

[41] All our hematites exhibit a thermal hysteresis. The WF → AF transformation in cooling occurs at a lower T_M than the AF → WF transformation on warming. The direction of approach to the transition should always be specified in reporting T_M; we have taken warming values as our standard. The hysteresis width ΔT_M is much greater in most submicron hematites than in natural MD crystals. Large ΔT_M values may result from widely distributed particle sizes. In very fine particles, the transition is thought to be inhibited by the lack of sufficiently large layers of rotated surface spins to initiate spin-flopping in the body of the particle. Lattice defects could have a similar stabilizing effect if they anchor extensive regions of surface spins.

[42] A field $\boldsymbol{H}$ applied in the basal plane stabilizes the WF phase, causing T_M to decrease linearly with increasing H. For standardized results, T_M should be measured in or extrapolated to zero field. However, the thermal hysteresis width ΔT_M does not seem to depend on field.

Acknowledgments

[43] MPMS and microVSM data were obtained at the Institute for Rock Magnetism (IRM), which is funded by the Earth Sciences Division of NSF, the Keck Foundation, and the University of Minnesota. We thank the editor John Tarduno and two anonymous referees for useful reviews and suggestions. This is IRM contribution number 0802. Our research was supported by the Natural Sciences and Engineering Research Council of Canada through grant A7709 to DJD.

References

Amin, N., and S. Arajs (1987), Morin transition of annealed submicron α-Fe_2O_3 particles, *Phys. Rev. B*, *35*, 4810–4811, doi:10.1103/PhysRevB.35.4810.

Anderson, P. W., F. R. Merritt, J. P. Remeika, and W. A. Yager (1954), Magnetic resonance in αFe_2O_3, *Phys. Rev.*, *93*, 717–718, doi:10.1103/PhysRev.93.717.

Bando, Y., M. Kiyama, N. Yamamoto, T. Takada, T. Shinjo, and H. Takaki (1965), The magnetic properties of α-Fe_2O_3, *J. Phys. Soc.*, *20*, 2086, doi:10.1143/JPSJ.20.2086.

Banerjee, S. K. (1971), New grain size limits for palaeomagnetic stability in haematite, *Nature Phys. Sci.*, *232*, 15–16.

Baruchel, J., G. Clark, B. K. Tanner, and B. E. Watts (1987), Neutron topographic investigation of the Morin transition in flux-grown crystals of α-Fe_2O_3, *J. Magn. Magn. Mater.*, *68*, 374–378, doi:10.1016/0304-8853(87)90016-3.

Bercoff, P. G., H. R. Bertorello, and M. I. Oliva (2007), Memory effect of ball-milled and annealed nanosized hematite, *Physica B*, *398*, 204–207, doi:10.1016/j.physb.2007.04.028.

Bødker, F., M. H. Hansen, C. B. Koch, K. Lefmann, and S. Mørup (2000), Magnetic properties of hematite nanoparticles, *Phys. Rev. B*, *61*, 6826–6838, doi:10.1103/PhysRevB.61.6826.

Chow, H., and F. Keffer (1974), Soft surface magnons and the first-order magnetic phase transition in antiferromagnetic hematite, *Phys. Rev. B*, *10*, 243–254, doi:10.1103/PhysRevB.10.243.

Dang, M.-Z., D. G. Rancourt, J. E. Dutrizac, G. Lamarche, and R. Provencher (1998), Interplay of surface conditions, particle size, stoichiometry, cell parameters, and magnetism in synthetic hematite-like materials, *Hyperfine Interact.*, *117*, 271–319, doi:10.1023/A:1012655729417.

de Boer, C. B., T. A. T. Mullender, and M. J. Dekkers (2001), Low-temperature behaviour of haematite: Susceptibility and magnetization increase on cycling through the Morin transition, *Geophys. J. Int.*, *146*, 201–216, doi:10.1046/j.0956-540x.2001.01443.x.

Donbaev, K. M., A. K. Zhetbaev, and M. K. Mukusheva (1993), New spin-reorientation transition in irradiated single crystal hematite, *Phys. Status Solidi B*, *176*, 219–226, doi:10.1002/pssb.2221760121.

Flanders, P. J. (1969), Spin axis rotation in hematite, *J. Appl. Phys.*, *40*, 1247–1248, doi:10.1063/1.1657614.

Flanders, P. J., and W. J. Schuele (1964), Anisotropy in the basal plane of hematite single crystals, *Philos. Mag.*, *9*, 485–490, doi:10.1080/14786436408222959.

Frandsen, C., and S. Mørup (2005), Spin rotation in α-Fe_2O_3 nanoparticles by interparticle interactions, *Phys. Rev. Lett.*, *94*, 027202(1)–027202(4).

Frandsen, C., et al. (2005), Oriented attachment and exchange coupling of α-Fe_2O_3 nanoparticles, *Phys. Rev. B*, *72*(7), 214,406(1)–214,406(7).

Gallagher, P. K., and E. M. Gyorgy (1969), Morin transition and lattice spacing of hematite as a function of particle size, *Phys. Rev.*, *180*, 622–623, doi:10.1103/PhysRev.180.622.

Gallon, T. E. (1968), The ferromagnetic domain structure of haematite, *Proc. R. Soc. London, Ser. A*, *303*, 511–524, doi:10.1098/rspa.1968.0066.

Gee, S.-H., Y.-K. Hong, J. C. Sur, D. W. Erickson, M. H. Park, and F. Jeffers (2004), Spin orientation of hematite (α-Fe_2O_3) nanoparticles during the Morin transition, *IEEE Trans. Magn.*, *40*, 2691–2693, doi:10.1109/TMAG.2004.832253.

Goya, G. F., M. Veith, R. Rapalavicuite, H. Shen, and S. Mathur (2005), Thermal hysteresis of spin reorientation at the Morin transition in alkoxide derived hematite nanoparticles, *Appl. Phys. A*, *80*, 1523–1526, doi:10.1007/s00339-003-2381-4.

Haigh, G. (1957a), The effect of added titanium and aluminium on the magnetic behaviour of α ferric oxide, *Philos. Mag.*, *2*, 505–520, doi:10.1080/14786435708243840.

Haigh, G. (1957b), Observations on the magnetic transition in hematite at −15°C, *Philos. Mag.*, *2*, 877–890, doi:10.1080/14786435708242726.

Hansen, M. F., F. Bødker, S. Mørup, K. Lefmann, K. N. Clausen, and P-.A. Lindgård (1997), Dynamics of magnetic

nanoparticles studied by neutron scattering, *Phys. Rev. Lett.*, *79*, 4910–4913, doi:10.1103/PhysRevLett.79.4910.

Hönigschmid, J., and G. Will (1979), A neutron diffraction investigation of the H–T phase diagram of α-Fe_2O_3, *Phys. Status Solidi*, *53*, 557–563, doi:10.1002/pssa.2210530219.

Klausen, S. N., et al. (2003), An inelastic neutron scattering study of hematite nanoparticles, *J. Magn. Magn. Mater.*, *266*, 68–78, doi:10.1016/S0304-8853(03)00457-8.

Kletetschka, G., and P. J. Wasilewski (2002), Grain size limit for SD hematite, *Earth Planet. Sci. Lett.*, *129*, 173–179.

Kuhn, L. T., K. Lefmann, C. R. H. Bahl, S. Hyborg Ancona, and P.-A. Lindgård (2006), Neutron study of magnetic excitations in 8-nm α-Fe_2O_3 nanoparticles, *Phys. Rev.*, *74*, 184406–1–184406–9.

Kündig, W., H. Bömmel, G. Constabaris, and R. H. Lindquist (1966), Some properties of supported small α-Fe_2O_3 particles determined with the Mössbauer effect, *Phys. Rev.*, *142*, 327–333, doi:10.1103/PhysRev.142.327.

Labushkin, V. G., N. N. Faleev, V. A. Figin, and A. S. Tsaprilov (1976), X-ray diffraction investigations of hematite single crystals. Phase transition from weakly ferromagnetic to pure antiferromagnetic state, *Sov. Phys. Solid State*, *18*, 1658–1659.

Le Gall, H., C. Leycuras, D. Minella, E. G. Rudashewsky, and V. S. Merkoulov (1977), Anomalous evolution of the magnetic and magnetooptical properties of hematite at temperature near and lower than the Morin phase transition, *Physica B*, *86–88*, 1223–1225, doi:10.1016/0378-4363(77)90855-5.

Liebermann, R. C., and S. K. Banerjee (1971), Magnetoelastic interactions in hematite: Implications for geophysics, *J. Geophys. Res.*, *76*, 2735–2756, doi:10.1029/JB076i011p02735.

Morin, F. J. (1950), Magnetic susceptibility of α-Fe_2O_3 and α-Fe_2O_3 with added titanium, *Phys. Rev.*, *78*, 819–820, doi:10.1103/PhysRev.78.819.2.

Morrish, A. H. (1994), *Canted Antiferromagnetism: Hematite*, 192 pp., World Sci, Singapore.

Morrish, A. H., G. B. Johnston, and N. A. Curry (1963), Magnetic transition in pure and Ga doped α-Fe_2O_3, *Phys. Lett.*, *7*, 177–178, doi:10.1016/0031-9163(63)90372-X.

Muench, G. H., S. Arajs, and E. Matijeviæ (1985), The Morin transition in small α-Fe_2O_3 particles, *Phys. Status Solidi A*, *92*, 187–192, doi:10.1002/pssa.2210920117.

Murad, E., and J. Cashion (2004), *Mössbauer Spectroscopy of Environmental Materials and Their Utilization*, Kluwer Acad., Boston.

Nathans, R., S. J. Pickart, H. A. Alperin, and P. J. Brown (1964), Polarized- neutron study of hematite, *Phys. Rev. A*, *136*, 1641–1647, doi:10.1103/PhysRev.136.A1641.

Nininger, R. C., and D. Schroeer (1978), Mössbauer studies of the Morin transition in bulk and microcrystalline α-Fe_2O_3, *J. Phys. Chem. Solids*, *39*, 137–144, doi:10.1016/0022-3697(78)90213-5.

Özdemir, Ö., and D. J. Dunlop (2002), Thermoremanence and stable memory of single-domain hematites, *Geophys. Res. Lett.*, *29*(18), 1877, doi:10.1029/2002GL015597.

Özdemir, Ö., and D. J. Dunlop (2005), Thermoremanent magnetization of multidomain hematite, *J. Geophys. Res.*, *110*, B09104, doi:10.1029/2005JB003820.

Özdemir, Ö., and D. J. Dunlop (2006), Magnetic memory and coupling between spin-canted and defect magnetism in hematite, *J. Geophys. Res.*, *111*, B12S03, doi:10.1029/2006JB004555.

Parpia, D. Y., M. Safa, B. K. Tanner, and G. F. Clark (1987), Synchrotron X-ray topography observation of the Morin transition in highly perfect crystals of haematite, *Phys. Status Solidi A*, *103*, 263–271, doi:10.1002/pssa.2211030130.

Ruskov, T., T. Tomov, and S. Georgiev (1976), Mössbauer investigation of the Morin transition in hematite, *Phys. Status Solidi A*, *37*, 295–302, doi:10.1002/pssa.2210370137.

Schetinkin, S. A., E. Wheeler, V. V. Kvardakov, M. Schlenker, and J. Baruchel (2003), Observation of the phase coexistence in α-Fe_2O_3 at the Morin transition by synchrotron radiation white beam section topography, *J. Phys. D Appl. Phys.*, *36*, A118–A121, doi:10.1088/0022-3727/36/10A/324.

Schroeer, D., and R. C. Nininger (1967), Morin transition in α-Fe_2O_3 microcrystals, *Phys. Rev. Lett.*, *19*, 632–634, doi:10.1103/PhysRevLett.19.632.

Shapira, Y. (1969), Ultrasonic behavior near the spin-flop transition of hematite, *Phys. Rev.*, *184*, 589–600, doi:10.1103/PhysRev.184.589.

Shull, C. G., W. A. Strauser, and E. O. Wollan (1951), Neutron diffraction by paramagetic and antiferromagnetic substances, *Phys. Rev.*, *83*, 333–345, doi:10.1103/PhysRev.83.333.

Sorescu, M., R. A. Brand, D. Mihaila-Tarabasanu, and L. Diamandescu (1999), The crucial role of particle morphology in the magnetic properties of haematite, *J. Appl. Phys.*, *85*, 5546–5548, doi:10.1063/1.369890.

Suber, L., et al. (1998), Structural and magnetic properties of α-Fe_2O_3 nanoparticles, *Appl. Organomet. Chem.*, *12*, 347–351, doi:10.1002/(SICI)1099-0739(199805)12:5<347::AID-AOC729>3.0.CO;2-G.

Vandenberghe, R. E., E. Van San, E. De Grave, and G. M. Da Costa (2001), About the Morin transition in hematite in relation with particle size and aluminium substitution, *Czech. J. Phys.*, *51*, 663–675, doi:10.1023/A:1017697715646.

Vlasov, K. B., E. A. Rozenberg, V. I. Timoshchuk, and Y. G. Smorodinskii (1986), Observation of a thermal hysteresis of the magnetization of a hematite single crystal near the Morin transition, *Sov. Phys. Solid State*, *28*, 1851–1853.

Williamson, D. L., E. L. Venturini, R. A. Graham, and B. Morosin (1986), Morin transition of shock-modified hematite, *Phys. Rev. B*, *34*, 1899–1907, doi:10.1103/PhysRevB.34.1899.

Zysler, R. D., D. Fiorani, A. M. Testa, L. Suber, E. Agostinelli, and M. Godinho (2003), Size dependence of the spin-flop transition in hematite nanoparticles, *Phys. Rev. B*, *68*(4), 212408(1)–212408(4).